ACS APPLIED MATERIALS & INTERFACES

Letter

www.acsami.org

An Approach to Prepare Polyethylenimine Functionalized Silica-Based Spheres with Small Size for siRNA Delivery

Meihua Yu,[†] Yuting Niu,[†] Yannan Yang,[†] Sandy Budi Hartono,[†] Jie Yang,[†] Xiaodan Huang,[†] Peter Thorn,[‡] and Chengzhong Yu*[,†]

[†]Australian Institute for Bioengineering and Nanotechnology and [‡]School of Biomedical Sciences, The University of Queensland, Brisbane, QLD 4072, Australia

Supporting Information

ABSTRACT: A novel approach has been developed to prepare polyethylenimine functionalized hybrid silica spheres with a diameter of ~10 nm, which show excellent delivery efficiency of siRNA into osteosarcoma cancer cells and human colon cancer cells with a significant cell inhibition comparable to commercial agents.

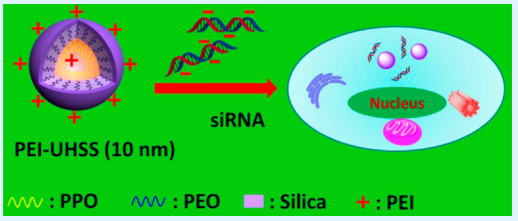

KEYWORDS: *silica nanoparticles, siRNA, surface modification, polyethylenimine, gene delivery*

Since the first report of long double-stranded ribonucleic acid (dsRNA) mediated gene silencing in worms in 1998,[1] RNA interference technology has already been regarded as a promising therapeutic approach to treat various diseases by inhibiting specific disease related gene expression.[2] The negative charge and big molecular size of small interfering RNA (siRNA) impair its accessibility to the cells. To achieve the gene silencing efficiency of siRNA, researchers have developed effective intracellular delivery systems including viral or nonviral vectors to exploit the therapeutic potential of siRNA.[3−5] Compared with viral vectors, synthetic nonviral siRNA delivery systems including organic[5] and inorganic nanoparticles[3] offer several advantages, such as easy fabrication and reduced immunogenicity. The development of new nonviral carriers is in great demand for gene silencing applications.

Silica-based nanoparticles (SiNPs) have attracted increasing attention for siRNA delivery because of their unique properties including tunable particle/pore size, stable and rigid framework, and feasibility of modification.[6−8] It has been well demonstrated that the cellular uptake performance of SiNPs is size-dependent; the smaller the particle, the higher endocytosis performance.[9] However, the conventional SiNPs tend to aggregate when the particle size is smaller than 50 nm. An emerging type of monodiperse SiNPs with small sizes from 6 to 30 nm has been developed by micelle templating approach.[10−12] Compared with conventional SiNPs, such small-sized SiNPs show enhanced cellular uptake performance and more uniform distribution in the cytoplasm of the cells both in monolayer and three-dimensional spheroid models.[13,14] Because of their unique advantages of excellent monodispersity and stability in aqueous media, small SiNPs have been utilized as bioimaging agents,[11] water-soluble electrochemiluminescence (ECL) materials[15] and dual nanosensors.[16] However, there is no report using small-sized SiNPs for siRNA delivery.

In previous studies, dimethyl-silane[10,13,14] or polyethylene glycol (PEG)-silane[12] was utilized to terminate the silicate condensation and prevent interparticle aggregation/growth to generate monodisperse small SiNPs. The protection groups are generally inert, making it difficult for the further modification of other functional groups. To facilitate the cellular uptake of the negatively charged siRNA, SiNPs need to be functionalized with positively charged amine groups,[17] poly-L-lysine (PLL),[18] or polyethylenimine (PEI).[19] Compared to other cationic groups, PEI has a higher endosomal escape capability, favoring a high gene silencing efficacy.[3,19] It remains a challenge to prepare PEI-modified monodisperse SiNPs with small sizes for siRNA delivery.

Herein, we report novel one-pot synthesis of epoxysilane functionalized ultrasmall hybrid silica spheres (Epoxy-UHSS) with a diameter of ~10 nm under phosphate-citrate buffer solution (pH 4.6) at room temperature. In this approach, a triblock copolymer $EO_{106}PO_{70}EO_{106}$ [Pluronic F127, EO is poly(ethylene oxide), PO is poly(propylene oxide)] is utilized as the template, and a mixture of tetramethyl orthosilane (TMOS) and diethoxy(3-glycidyloxypropyl)methylsilane (DGMS) are used as silica sources. As shown in Scheme 1, Epoxy-UHSS comprises a PPO core and epoxy-silane terminated silica/PEO shell, which can be easily covalently conjugated with PEI (PEI-UHSS) by nucleophilic addition to the epoxy groups. Different from previously reported methods,[10,12−14] our strategy, using a new precursor, leads to the grafting of both an inert alkyl group and a reactive group

Received: May 18, 2014
Accepted: September 3, 2014
Published: September 3, 2014

Scheme 1. Illustration of the Polyethyleneimine Conjugation Process on the Surface of Epoxy-UHSS, Followed by the siRNA Delivery into Cells

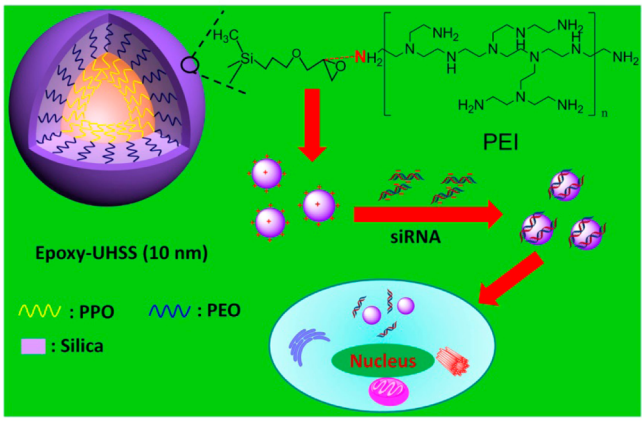

(epoxy), and eventually the successful preparation of PEI-modified monodisperse SiNPs with small sizes for siRNA delivery. This designed positively charged PEI-UHSS was proven to facilitate the cellular uptake of negatively charged siRNA by forming siRNA complexation via electrostatic interaction. PEI-UHSS demonstrated excellent delivery efficiency of a functional siRNA against polo-like kinase 1 (PLK1-siRNA) in osteosarcoma cancer cells (KHOS) and survivin-siRNA in human colon cancer cells (HCT-116) inducing a significant cell inhibition, which is comparable to a commercial product, Oligofectamine.

A representative transmission electron microscopy (TEM) image of Epoxy-UHSS is displayed in Figure 1a, which shows ultrasmall spherical core−shell particles with a uniform size. The core of Epoxy-UHSS is formed by the hydrophobic segment PPO of F127, showing low contrast under TEM observation. The shell is generated by the polymerization of silicate species in the hydrophilic PEO region, showing dark contrast. The average diameter was measured to be approximately 9.3 nm (see Figure S1a in the Supporting Information). The dynamic light scattering (DLS) measurement was further utilized to evaluate the size and dispersibility of Epoxy-UHSS. As shown in Figure S1b in the Supporting Information, Epoxy-UHSS shows a narrow size distribution curve with a small polydisperse index (PDI) value of 0.081 ± 0.006, suggesting that the Epoxy-UHSS are well-dispersed in aqueous solution. The hydrodynamic diameter of Epoxy-UHSS is 23.8 ± 0.7 nm, which is larger than that measured by TEM due to the surrounded water molecules.[20] Epoxy-UHSS solution is stable as a colloidal suspension over the period of this study (more than 10 months) (see Figure S1c in the Supporting Information).

It should be noted that the methyl group connected to silicon in DGMS (marked by red circle in its chemical structure in Figure S2 in the Supporting Information) is essential to obtain Epoxy-UHSS with excellent monodispersity. When DGMS was replaced by equal molar amount of (3-glycidyloxypropyl)trimethoxysilane (GPTMS, see Figure S2 in the Supporting Information) during the synthesis of Epoxy-UHSS, the small particles tend to aggregate to form big clusters (see Figure S3 in the Supporting Information).

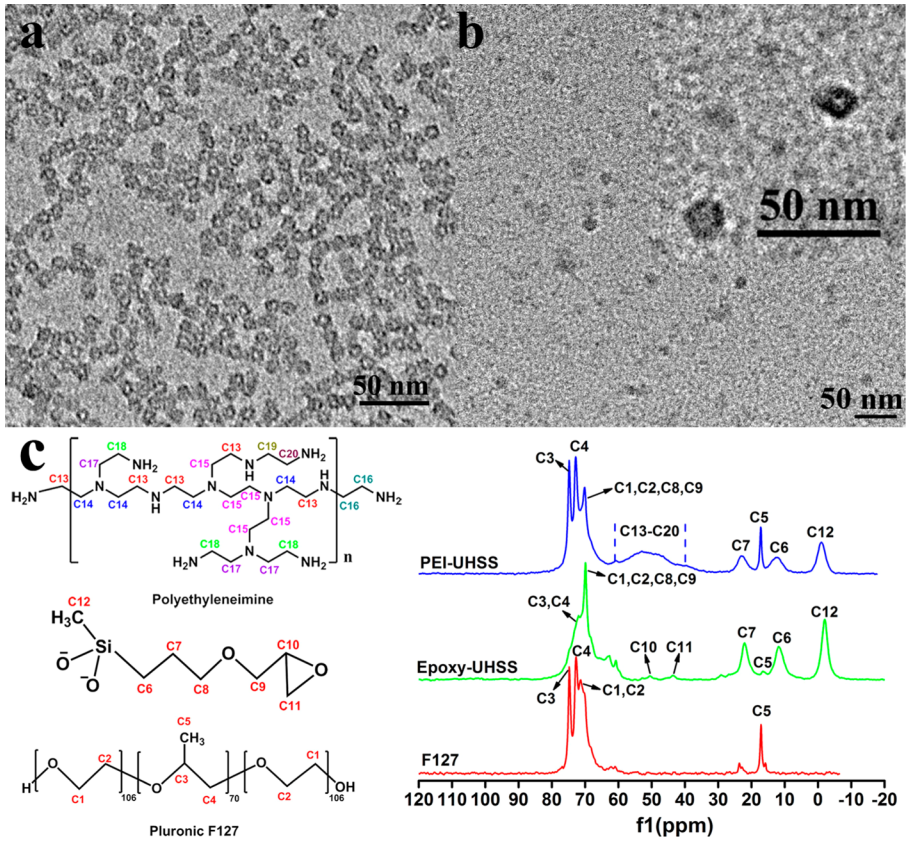

Figure 1. TEM images of (a) Epoxy-UHSS and (b) PEI-UHSS and (c) solid-state ^{13}C CPMAS NMR spectra of F127, Epoxy-UHSS, and PEI-UHSS.

dx.doi.org/10.1021/am503060n | ACS Appl. Mater. Interfaces 2014, 6, 15626−15631

In order to facilitate the cellular delivery of negatively charged siRNA, Epoxy-UHSS was modified with PEI (denoted as PEI-UHSS) via the nucleophilic reaction between epoxy groups and amino groups (see Scheme S1 in the Supporting Information).[18] From the TEM image (Figure 1b), it can be seen that PEI-UHSS have a spherical core−shell structure (inset of Figure 1b) with a uniform diameter of about 10 nm, similar to what observed in Epoxy-UHSS (Figure 1a). However, the shell structure of PEI-UHSS becomes vague, which may be caused by the coating of organic PEI polymer. A narrow size distribution (see Figure S4 in the Supporting Information) was observed in the DLS curve of PEI-UHSS, suggesting uniform particle size and high dispersity. The hydrodynamic diameter of PEI-UHSS is 13.3 ± 1.9 nm, close to that measured by TEM.

The chemical structures of organic species of the designed materials were investigated by solid state ^{13}C CPMAS NMR technique. As shown in Figure 1c, the well-resolved peaks in the spectrum of F127 are attributed to methane carbons C3 (74.7 ppm), methylene carbons C4 (72.7 ppm) and methyl carbons C5 (17.1 ppm) of PO chains, and methylene carbons C1 and C2 (71.4 ppm) of EO chains.[21] In the spectrum of Epoxy-UHSS, the intense peak at 70.0 ppm is assigned to methylene carbons in EO units, and the less defined broad peak centered at 72.0 ppm to the methylene carbons of PO units. A weak peak at 16.5 ppm is attributed to methyl carbons of PO units. Another two typical peaks at 50.5 and 43.7 ppm suggest the presence of the carbons C10 and C11 of the epoxide ring, respectively,[18] and the distinct peak at −2.0 ppm reveals the presence of methyl carbons C12 connected to silicon atoms. The characteristic peaks at 22.1 and 11.8 ppm are attributed to the methylene carbons C7, C6 close to silicon atoms, respectively. The other two methylene carbons C8 and C9 in epoxy-silane are overlapped by the carbons in EO chains. All the characteristic peaks confirm the chemical structure of epoxy/methyl-silane. According to different combinations of amine nearest neighbors (chemical structure of PEI, left top of Figure 1c), PEI has eight carbon peaks in the range of 38−60 ppm.[22] Besides the characteristic peaks coming from surfactant F127 and epoxy/methyl-silane, a very broad extra peak can be observed in the range of 38−60 ppm in the spectrum of PEI-UHSS, corresponding to the carbons in PEI.[23] On the basis of the reaction mechanism between the epoxy moiety of and primary amine groups, the epoxy ring will open to form CH_2−O−CH_2−CH(OH)−CH_2−NH-. The chemical shifts of C10 and C11 in epoxy-silane will be changed to ∼70 and 52 ppm, respectively,[24] which is overlapped by the typical carbons in the EO units and PEI, respectively.

The Zeta potential (see Figure S5 in the Supporting Information) and elemental analysis results (see Table S1 in the Supporting Information) further confirm the successful modification of PEI on Epoxy-UHSS. The grafted PEI weight percentage in PEI-UHSS is calculated to be ∼11.52% (see Table S1 in the Supporting Information).

To evaluate the cellular delivery performance of PEI-UHSS, e used the cyanine dye-labeled oligoDNA (Cy3-oligoDNA) was used as a model of nucleic acid entry into cells. As shown in Figure S6 in the Supporting Information, no Cy3 signals (red fluorescence) can be detected under confocal microsocpy when the cells are treated with Cy3-oligoDNA alone, indicating that nucleic acids themselves cannot enter into cells. In contrast, strong Cy3 signals can be observed within the cytoplasm of cells when PEI-UHSS are utilized to deliver Cy3-oligoDNA (Figure 2). These results demonstrate that the designed PEI-UHSS can efficiently deliver the negative charged genetic molecules into cells.

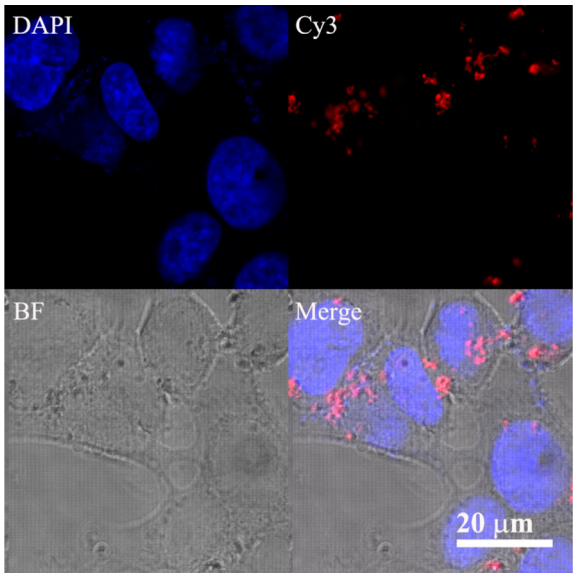

Figure 2. Confocal microscopy images of KHOS cells treated with Cy3-oligoDNA/PEI-UHSS.

The cytotoxicity of PEI-UHSS was evaluated in KHOS and human colon cancer cells (HCT-116). As shown in panels a and b in Figure 3, at the concentration of 10 μg/mL PEI-UHSS in two cell lines showed about 10% cell toxicity. This dosage was chosen for the following siRNA delivery studies.

A functional PLK1-siRNA was chosen to investigate the gene delivery efficiency of PEI-UHSS in KHOS cells. Before that, the protection of PLK1-siRNA against nuclease degradation was evaluated by measuring the percent increase in absorbance at 260 nm after RNase A treatment, as siRNA degradation results in a hyperchromic effect.[25,26] In our study, free PLK1-siRNA exhibited a 55% increase in absorbance at 260 nm (see Figure S7 in the Supporting Information), which is much higher than that of the complex of PEI-UHSS/PLK1-siRNA (28%). This result confirms that PEI-UHSS have the capacity to protect siRNA from rapid degradation by RNase A, which is important for successful gene delivery. It has been well reported that PLK1 gene is highly expressed in osteosarcoma cells and knockdown of PLK1 induces apoptosis of KHOS cells.[18,27] Another siRNA, S10-siRNA was chosen as a negative control, which silences human papillomavirus type 16 E6 gene expressed at only low levels in KHOS cells and therefore not expected to have large functional effects.[18] As displayed in Figure 3c, when PEI-UHSS is utilized to deliver PLK1-siRNA, the cell viability decreases in a dose-dependent manner (72, 55, and 43% at a dose of 25, 50, 100 nM, respectively). In contrast, only a small decrease in cell viability is seen when S10-siRNA is delivered into KHOS cells by PEI-UHSS. For comparison, a commercial transfection agent Oligofectamine, was chosen as a positive control. When Oligofectamine is used to deliver PLK1-siRNA, cell viability also shows a PLK1-siRNA dose-dependent behavior (51, 46, and 37% at a dose of 25, 50, 100 nM, respectively). Moreover, there is no significant difference (p = 0.196) in cell viability between PEI-UHSS and Oligofectamine with a PLK1-siRNA dose of 100 nM. The negative control,

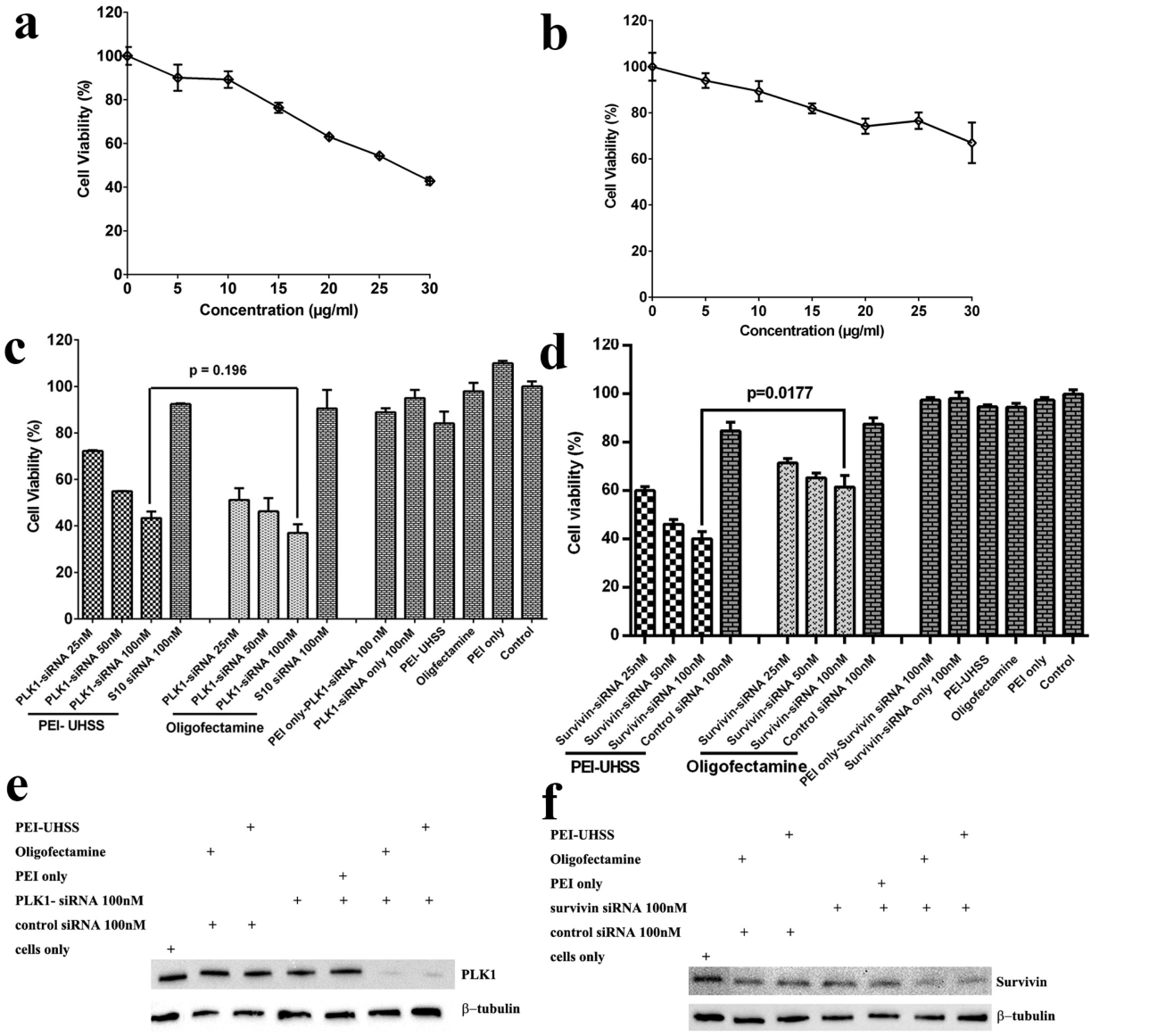

Figure 3. Cell viability of (a) KHOS and (b) HCT-116 cells after treated with PEI-UHSS at different concentrations; delivery efficiency of (c) PLK1-siRNA in KHOS cells and (d) survivin siRNA in HCT-116 cells; western-blot analysis of (e) PLK1 protein in KHOS cells and (f) survivin protein in HCT-116 cells.

delivering S10-siRNA by Oligofectamine, shows no effect on cell viability. To demonstrate the relative advantage of PEI-UHSS, we also investigated PLK1-siRNA delivery efficiency by PEI polymer only. The concentration of PEI used for PLK1-siRNA delivery was the same as that contained in PEI-UHSS, which was calculated from the dosage and PEI percentage of PEI-UHSS. PEI only shows only a slight cell inhibition, even at the highest PLK1-siRNA concentration (100 nM). In addition, all the tested carriers and PLK1-siRNA themselves do not show significant effects on cell viability. Compared to previously reported results where functionalized silica materials with larger sizes were utilized to deliver PLK1-siRNA,[18] the cell inhibition capacity in this study is relatively higher. These results demonstrate the excellent siRNA delivery efficiency of novel designed PEI-UHSS, which is comparable with the commercial agent.

The gene delivery efficiency of PEI-UHSS was further investigated in another functional siRNA, survivin-siRNA. Previous studies demonstrated that RNA interference of survivin led to a significant decrease in invasiveness and proliferation of HCT-116.[28] As displayed in Figure 3d, survivin-siRNA delivered by PEI-UHSS shows a dose-dependent behavior with a cell inhibition of 40%, 54% and 60% at the dose of 25, 50, 100 nM, respectively. When Oligofectamine is utilized to deliver survivin-siRNA, the cell proliferation is also inhibited in a survivin-siRNA dose-dependent behavior (29%, 35%, and 39% inhibition at the dose of 25, 50, 100 nM, respectively). However, there is a significant difference (p = 0.0177) in cell inhibition between PEI-UHSS and Oligofectamine with a survivin-siRNA dose of 100 nM. In contrast, survivin-siRNA only or delivered by PEI only showed a negligible cell inhibition with a concentration of 100 nM. The negative control siRNA delivered by PEI-UHSS or Oligofectamine shows no effect on cell inhibition.

We further studied the knockdown efficiency of PLK1 protein in KHOS cells and survivin protein in HCT-116 cells by Western blot analysis. As shown in Figure 3e, upon incubation with PLK1-siRNA delivered by PEI-UHSS and

Oligofectamine, PLK1 protein expression was significantly suppressed in KHOS cells, compared to cells only group. Similarly, survivin protein expression in HCT-116 was obviously knocked down when survivin siRNA was delivered by PEI-UHSS and Oligofectamine (Figure 3f). In contrast, there is no significant PLK1 or survivin protein suppression in other groups (Figure 3e, f). The gene silencing at PLK1 and survivin protein is highly efficient with PEI-UHSS delivery system, which induces apoptosis and consequently cell death of KHOS and HCT-116, respectively.

In summary, a novel approach has been developed to generate polyethylenimine functionalized ultrasmall hybrid silica spheres (PEI-UHSS) with a diameter of ∼10 nm. PEI-UHSS have been demonstrated to an excellent vector to efficiently deliver siRNA into cells, which is comparable with commercial agents. This approach could be helpful to design efficient siRNA delivery systems to improve gene therapy efficacy.

■ ASSOCIATED CONTENT

Supporting Information

Experimental section, DLS, digital images, TEM figures, Zeta potential values, elemental analysi,s and confocal images. This material is available free of charge via the Internet at http://pubs.acs.org.

■ AUTHOR INFORMATION

Corresponding Author

*E-mail: c.yu@uq.edu.au.

Notes

The authors declare no competing financial interest.

■ ACKNOWLEDGMENTS

We acknowledge the support from the Australian Research Council, the Australian National Fabrication Facility and the Australian Microscopy and Microanalysis Research Facility at the Centre for Microscopy and Microanalysis, The University of Queensland. We thank Dr. Ekaterina Strounina for the ^{13}C NMR technical help from Centre for Advanced Imaging, The University of Queensland.

■ REFERENCES

(1) Fire, A.; Xu, S. Q.; Montgomery, M. K.; Kostas, S. A.; Driver, S. E.; Mello, C. C. Potent and Specific Genetic Interference by Double-Stranded RNA in Caenorhabditis Elegans. *Nature* **1998**, *391*, 806−811.

(2) Kurreck, J. RNA Interference: From Basic Research to Therapeutic Applications. *Angew. Chem., Int. Ed.* **2009**, *48*, 1378−1398.

(3) Sokolova, V.; Epple, M. Inorganic Nanoparticles as Carriers of Nucleic Acids into Cells. *Angew. Chem., Int. Ed.* **2008**, *47*, 1382−1395.

(4) Stewart, S. A.; Dykxhoorn, D. M.; Palliser, D.; Mizuno, H.; Yu, E. Y.; An, D. S.; Sabatini, D. M.; Chen, I. S. Y.; Hahn, W. C.; Sharp, P. A.; Weinberg, R. A.; Novina, C. D. Lentivirus-Delivered Stable Gene Silencing by RNAi in Primary Cells. *RNA-Publ. RNA Soc.* **2003**, *9*, 493−501.

(5) Urban-Klein, B.; Werth, S.; Abuharbeid, S.; Czubayko, F.; Aigner, A. RNAi-Mediated Gene-targeting Through Systemic Application of Polyethylenimine (PEI)-Complexed siRNA In Vivo. *Gene Ther.* **2005**, *12*, 461−466.

(6) Chen, A. M.; Zhang, M.; Wei, D. G.; Stueber, D.; Taratula, O.; Minko, T.; He, H. X. Co-delivery of Doxorubicin and Bcl-2 siRNA by Mesoporous Silica Nanoparticles Enhances the Efficacy of Chemotherapy in Multidrug-Resistant Cancer Cells. *Small* **2009**, *5*, 2673−2677.

(7) Xia, T. A.; Kovochich, M.; Liong, M.; Meng, H.; Kabehie, S.; George, S.; Zink, J. I.; Nel, A. E. Polyethyleneimine Coating Enhances the Cellular Uptake of Mesoporous Silica Nanoparticles and Allows Safe Delivery of siRNA and DNA Constructs. *ACS Nano* **2009**, *3*, 3273−3286.

(8) Meng, H. A.; Liong, M.; Xia, T. A.; Li, Z. X.; Ji, Z. X.; Zink, J. I.; Nel, A. E. Engineered Design of Mesoporous Silica Nanoparticles to Deliver Doxorubicin and P-Glycoprotein siRNA to Overcome Drug Resistance in a Cancer Cell Line. *ACS Nano* **2010**, *4*, 4539−4550.

(9) Lu, F.; Wu, S. H.; Hung, Y.; Mou, C. Y. Size Effect on Cell Uptake in Well-Suspended, Uniform Mesoporous Silica Nanoparticles. *Small* **2009**, *5*, 1408−1413.

(10) Huo, Q. S.; Liu, J.; Wang, L. Q.; Jiang, Y. B.; Lambert, T. N.; Fang, E. A New Class of Silica Cross-Linked Micellar Core-Shell Nanoparticles. *J. Am. Chem. Soc.* **2006**, *128*, 6447−6453.

(11) Tan, H.; Liu, N. S.; He, B. P.; Wong, S. Y.; Chen, Z. K.; Li, X.; Wang, J. Facile Synthesis of Hybrid Silica Nanocapsules by Interfacial Templating Condensation and Their Application in Fluorescence Imaging. *Chem. Commun.* **2009**, 6240−6242.

(12) Ma, K.; Sai, H.; Wiesner, U. Ultrasmall Sub-10 nm Near-Infrared Fluorescent Mesoporous Silica Nanoparticles. *J. Am. Chem. Soc.* **2012**, *134*, 13180−13183.

(13) Zhu, J.; Tang, J. W.; Zhao, L. Z.; Zhou, X. F.; Wang, Y. H.; Yu, C. Z. Ultrasmall, Well-Dispersed, Hollow Siliceous Spheres with Enhanced Endocytosis Properties. *Small* **2010**, *6*, 276−282.

(14) Yu, M. H.; Karmakar, S.; Yang, J.; Zhang, H. W.; Yang, Y. N.; Thorn, P.; Yu, C. Z. Facile Synthesis of Ultra-Small Hybrid Silica Spheres for Enhanced Penetration in 3D Glioma Spheroids. *Chem. Commun.* **2014**, *50*, 1527−1529.

(15) Zanarini, S.; Rampazzo, E.; Bonacchi, S.; Juris, R.; Marcaccio, M.; Montalti, M.; Paolucci, F.; Prodi, L. Iridium Doped Silica-PEG Nanoparticles: Enabling Electrochemiluminescence of Neutral Complexes in Aqueous Media. *J. Am. Chem. Soc.* **2009**, *131*, 14208−14209.

(16) Wang, X. D.; Stolwijk, J. A.; Lang, T.; Sperber, M.; Meier, R. J.; Wegener, J.; Wolfbeis, O. S. Ultra-Small, Highly Stable, and Sensitive Dual Nanosensors for Imaging Intracellular Oxygen and pH in Cytosol. *J. Am. Chem. Soc.* **2012**, *134*, 17011−17014.

(17) Na, H. K.; Kim, M. H.; Park, K.; Ryoo, S. R.; Lee, K. E.; Jeon, H.; Ryoo, R.; Hyeon, C.; Min, D. H. Efficient Functional Delivery of siRNA using Mesoporous Silica Nanoparticles with Ultralarge Pores. *Small* **2012**, *8*, 1752−1761.

(18) Hartono, S. B.; Gu, W. Y.; Kleitz, F.; Liu, J.; He, L. Z.; Middelberg, A. P. J.; Yu, C. Z.; Lu, G. Q.; Qiao, S. Z. Poly-L-lysine Functionalized Large Pore Cubic Mesostructured Silica Nanoparticles as Biocompatible Carriers for Gene Delivery. *ACS Nano* **2012**, *6*, 2104−2117.

(19) Niu, Y.; Yu, M.; Hartono, S. B.; Yang, J.; Xu, H.; Zhang, H.; Zhang, J.; Zou, J.; Dexter, A.; Gu, W.; Yu, C. Nanoparticles Mimicking Viral Surface Topography for Enhanced Cellular Delivery. *Adv. Mater.* **2013**, *25*, 6233−6237.

(20) Jung, H. S.; Moon, D. S.; Lee, J. K. Quantitative Analysis and Efficient Surface Modification of Silica Nanoparticles. *J. Nanomater.* **2012**, *2012*, 593471.

(21) Yang, C. M.; Zibrowius, B.; Schmidt, W.; Schuth, F. Stepwise Removal of the Copolymer Template from Mesopores and Micropores in SBA-15. *Chem. Mater.* **2004**, *16*, 2918−2925.

(22) Idris, S. A.; Mkhatresh, O. A.; Heatley, F. Assignment of H-1 NMR Spectrum and Investigation of Oxidative Degradation of Poly(ethylenimine) Using H-1 and C-13 1-D and 2-D NMR. *Polym. Int.* **2006**, *55*, 1040−1048.

(23) Lee, H.; Sung, D.; Veerapandian, M.; Yun, K.; Seo, S. W. PEGylated Polyethyleneimine Grafted Silica Nanoparticles: Enhanced Cellular Uptake and Efficient siRNA Delivery. *Anal. Bioanal. Chem.* **2011**, *400*, 535−545.

(24) Sales, J. A. A.; Prado, A. G. S.; Airoldi, C. The Incorporation of Propane-1,3-diamine into Silylant Epoxide Group Through Hornogeneous and Heterogeneous Routes. *Polyhedron* **2002**, *21*, 2647−2651.

(25) Yu, S. S.; Lau, C. M.; Barham, W. J.; Onishko, H. M.; Nelson, C. E.; Li, H. M.; Smith, C. A.; Yull, F. E.; Duvall, C. L.; Giorgio, T. D.

Macrophage-Specific RNA Interference Targeting via ″Click″, Mannosylated Polymeric Micelles. *Mol. Pharmaceutics* **2013**, *10*, 975−987.
(26) Kirkland-York, S.; Zhang, Y. L.; Smith, A. E.; York, A. W.; Huang, F. Q.; McCormick, C. L. Tailored Design of Au Nanoparticle-siRNA Carriers Utilizing Reversible Addition - Fragmentation Chain Transfer Polymers. *Biomacromolecules* **2010**, *11*, 1052−1059.
(27) Yamaguchi, U.; Honda, K.; Satow, R.; Kobayashi, E.; Nakayama, R.; Ichikawa, H.; Shoji, A.; Shitashige, M.; Masuda, M.; Kawai, A.; Chuman, H.; Iwamoto, Y.; Hirohashi, S.; Yamada, T. Functional Genome Screen for Therapeutic Targets of Osteosarcoma. *Cancer Sci.* **2009**, *100*, 2268−2274.
(28) Gao, F.; Zhang, Y. Q.; Yang, F.; Wang, P.; Wang, W. J.; Su, Y.; Luo, W. R. Survivin Promotes the Invasion of Human Colon Carcinoma Cells by Regulating the Expression of MMP-7. *Mol. Med. Rep.* **2014**, *9*, 825−830.